

Evidence for two distinct spin relaxation mechanisms in ‘hot’ spin ice $\text{Ho}_2\text{Ti}_2\text{O}_7$

G. Ehlers^{† ‡}, A. L. Cornelius[§], T. Fennell^{||}, M. Koza[¶], S. T. Bramwell⁺, and J. S. Gardner^{* ‡}

[†] SNS Project, Oak Ridge National Laboratory, 701 Scarboro Road, Oak Ridge, TN 37830, USA

[§] Physics Department, University of Nevada Las Vegas, Las Vegas, NV 89154-4002, USA

^{||} The Royal Institution of Great Britain, 21 Abermarle Street, London W1X 4BS, UK

[¶] Institut Laue-Langevin, 6 rue Jules Horowitz, 38042 Grenoble, France

⁺ Department of Chemistry, University College London, 20 Gordon Street, London WC1H 0AJ, UK

^{*} NIST Center for Neutron Research, NIST, Gaithersburg, MD 20899-8562, USA

[‡] Physics Department, Brookhaven National Laboratory, Upton, New York 11973, USA

Abstract. Neutron scattering and ac-susceptibility techniques have been performed on the spin ice material $\text{Ho}_2\text{Ti}_2\text{O}_7$ to study the spin relaxation in the ‘hot’ paramagnetic phase ($T > 1$ K). Neutron spin echo (NSE) proves that above $T \simeq 15$ K the spin dynamics is generated by a thermally activated single-ion process. At lower temperatures ($T < 15$ K) it cannot account for the spin dynamics found in ac-susceptibility measurements, and it is inferred that a second, slower process, with different thermal signature dominates. We suggest that this may be a quantum-mechanical process, probably tunneling between different spin states separated by a large energy barrier.

PACS numbers: 75.50 Dd, 75.40 Gb, 75.25 +z

[‡] To whom correspondence should be addressed (ehlersg@ornl.gov)

1. Introduction

Ever since the discovery of holmium titanate, $\text{Ho}_2\text{Ti}_2\text{O}_7$ (HTO), as a topologically frustrated *ferromagnet*, it has fascinated researchers who appreciate the beauty of frustrated magnets [1, 2, 3]. It was further realized that the related compounds dysprosium titanate, $\text{Dy}_2\text{Ti}_2\text{O}_7$ (DTO), [4, 5] and holmium stannate, $\text{Ho}_2\text{Sn}_2\text{O}_7$ (HSO), [6, 7] show similar low-temperature properties. It was the similarity of the low-temperature spin arrangement in these substances to the proton disorder in water ice that gave spin ice its name. Geometrical frustration occurs in a magnet when the spatial arrangement of the magnetic moments (“spins”) combined with their specific near neighbour interactions J inhibits the formation of a ‘simple’ ordered collinear ground state at low temperature, $T \leq J$ (for reviews, see [8, 9]). Spins with antiferromagnetic (afm) coupling to near neighbours, residing in building units of triangles or tetrahedra, are well known examples. Generally, as a result of the frustration, there is a lack of long range order, and the spins show glassy-like freezing, for example in $\text{Y}_2\text{Mo}_2\text{O}_7$ [10, 11], or may even stay dynamic down to the lowest accessible temperatures, for example in $\text{Tb}_2\text{Ti}_2\text{O}_7$ [12]. Some systems nevertheless show magnetic order, but often at a temperature considerably lower than the intrinsic energy scale (indicated by the paramagnetic Curie-Weiss temperature). The ordering pattern often shows signs of the frustration. For example, in $\text{Gd}_2\text{Ti}_2\text{O}_7$ [13], TbNiAl [14] and CsCoBr_3 [15, 16, 17] dynamic (paramagnetic) spins coexist with ordered spins.

It had long been thought that afm couplings between nearest neighbours are a necessary ingredient to frustration in magnets. The discovery of a frustrated *ferromagnet* thus came somewhat as a surprise. In HTO, where the rare earth ions occupy a lattice of corner-sharing tetrahedra, frustration is created by the splitting of the ionic states in the crystalline electric field (CEF). The single ion ground state is an almost pure $|J, M_J\rangle = |8, \pm 8\rangle$ doublet which is separated by 20.4 meV \sim 240 K from the first excited state [18]. The strong Ising anisotropy forces each spin to point into the centre of one of the two tetrahedra it belongs to. The energy a pair of spins can gain by mutual alignment, in contrast, is some 2 orders of magnitude smaller: The dipolar energy is $D_{\text{nn}} = +2.4$ K [3], the near neighbour exchange was estimated to $J_{\text{nn}} = -0.5$ K [19]. A macroscopic ground state degeneracy results, as any state which obeys the ice-rule ‘two in - two out’ for all tetrahedra is a ground state, and the spins freeze below $T \simeq 1$ K in a non-collinear disordered pattern. Absence of long range order has been confirmed down to $T = 50$ mK [20].

In this paper we mainly report on the spin dynamics of HTO at temperatures above the freezing. This study was motivated by the frequency-dependent susceptibility investigations of Matsuhira *et al.* [6, 21] and Snyder *et al.* [22, 23], which revealed a rich spectrum of dynamics in the spin ice materials. All spin ice compounds show a distinct susceptibility peak at $T \simeq 1$ K which gives a frequency shift consistent with an activation energy of $\simeq 20$ K. For DTO [21, 22, 23] another peak in the ac susceptibility at $T \simeq 15$ K is consistent with a thermally activated relaxation process characterized by

an activation barrier of $\simeq 210$ K. However, the 15 K peak was not reported for the Ho compounds, suggesting that there may be important differences between the different spin ice materials.

2. Experimental

As it turns out, to study the dynamics of spin ice by neutron scattering, one has to resort to high energy resolution, because in the interesting temperature range ($T \simeq 15$ K and below) the spin dynamics is very slow. This calls for the Neutron Spin Echo (NSE) technique, which offers by far the highest energy resolution.

NSE is a fairly advanced technique to study spatial and temporal correlation functions in matter. The quantity one measures is the intermediate scattering function $S(q, t)$. Accessible ranges are $\sim 10^{-2} \text{ \AA}^{-1} \leq q \leq \sim 3 \text{ \AA}^{-1}$ and $\sim 10^{-14} \text{ s} \leq t \leq \sim 10^{-7} \text{ s}$, respectively. An experiment involves a polarized neutron beam, with the neutron polarization perpendicular to the magnetic guide field. The neutron spins precess in two identical fields placed before and after the sample. In case of strictly elastic scattering the original neutron beam polarization is restored at the end, because all neutrons will end up with a net zero difference in the number of precessions (before and after the sample). The actual number of precessions performed by an individual neutron is proportional to the wavelength, which is typically spread by 16% FWHM around the mean value. Generally, a small inelasticity in the scattering will therefore be detected by a loss in the final neutron beam polarization. References to the method and its applications to spin glasses, magnetic nanoparticles, and other frustrated magnets are available [24, 25, 26].

In this experiment, the NSE spectrometer IN11 was used in its wide angle multidetector configuration. The neutron wavelength was $\lambda = 5.5 \text{ \AA}$, and a q range of $0.5 \text{ \AA}^{-1} \leq q \leq 1.6 \text{ \AA}^{-1}$ was covered by two positions of the detector bank. Instrumental resolution was measured using a magnetic sample whose spins are frozen at low temperature. In order to get the normalized intermediate scattering function $S(q, t)$, the spin echo experiment includes xyz -polarization analysis [27]. This procedure separates magnetic scattering from other sorts (spin incoherent and nuclear) of scattering. Thus, the elastic magnetic scattering intensity is obtained as a side benefit (though with bad q resolution, because of the 16% wavelength distribution of the incident beam).

To extend the study to higher temperature, neutron time-of-flight (TOF) spectra were collected at IN6 at the standard wavelength $\lambda = 5.9 \text{ \AA}$, which gives a width of the quasielastic line of $\Delta = 50 \mu\text{eV}$. The q range of the quasielastic scattering was $0.2 \text{ \AA}^{-1} \leq q \leq 2.1 \text{ \AA}^{-1}$. A vanadium sample was used as a reference. Standard data corrections for resolution and background were applied. To obtain the relaxation time from the TOF data, the resolution was deconvoluted and a fit to a Lorentzian line shape was performed. The relaxation time is then given by $\tau (\text{ns}) = 1.317/\text{FWHM} (\mu\text{eV})$.

AC susceptibility measurements have been performed on a single-crystal sample of HTO in an external field of up to 1 T applied along a cubic $\langle 111 \rangle$ direction.

3. Results

3.1. neutron scattering

Figure 1 (top panel) shows the normalized intermediate scattering function $S(q, t)$ at different temperatures as obtained from the NSE experiment. The spin relaxation was found to be q -independent (lower panels in Figure 1).

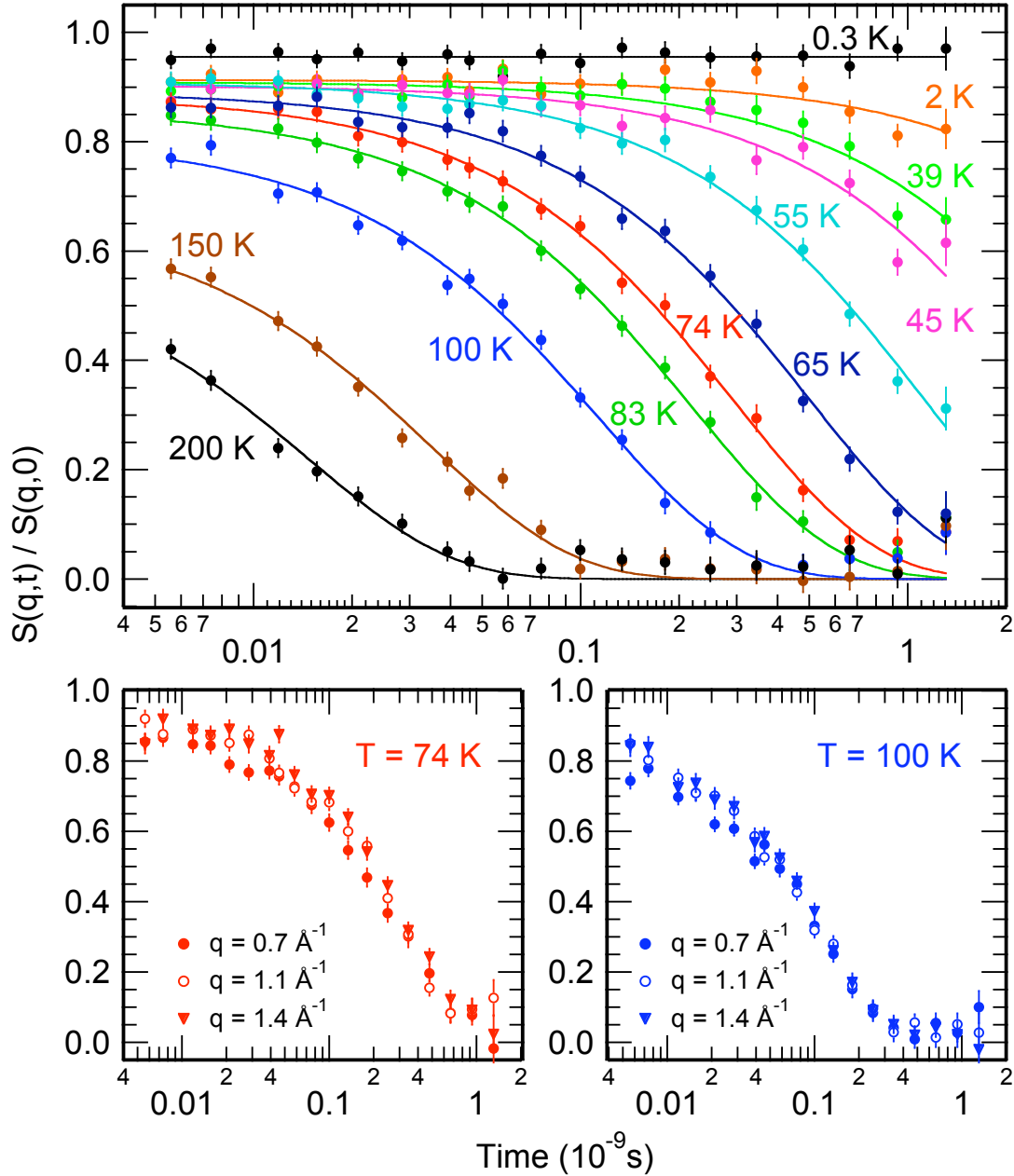


Figure 1. Top panel: the normalized intermediate scattering function $S(q, t)/S(q, 0)$ as measured at IN11, integrated in the range $0.5 \text{ \AA}^{-1} \leq q \leq 1.0 \text{ \AA}^{-1}$. Bottom panels: as a function of q , showing negligible q dependence.

At all temperatures between 0.3 K and 200 K the intermediate scattering function can be fitted with excellent precision to a simple exponential

$$\frac{S(q, t)}{S(q, 0)} = A \cdot \exp(-t/\tau(T)), \quad (1)$$

where $A = 0.91 \pm 0.01$ in the temperature range between $\simeq 2$ K and $\simeq 50$ K. The fact that $A < 1$ is discussed further below.

Figure 2 extends the quasielastic scattering to higher temperature, showing that it can be described equally well with the corresponding model in ω space (Lorentzian convoluted with resolution). The right panel of Figure 2 shows the temperature dependence of the resulting relaxation time $\tau(T)$ in an Arrhenius plot. A line fit yields $\tau_0 = 4.5 \pm 0.7 \times 10^{-3}$ ns, corresponding to an attempt frequency $\Gamma_0 = 1/2\tau_0 = 1.1 \pm 0.2 \times 10^{11}$ Hz, and an activation energy of $E_a = 293 \pm 12$ K. Note, that the data actually don't follow an Arrhenius law precisely (which would give a straight line in the figure). Deviations at low temperature could be due to a systematic error: Here the relaxation clearly goes out of the spin echo time window. At high temperature deviations may be due to the fact that spin ice is not an ideal two level system, rather, there are more crystal field levels close to the first excited level [18].

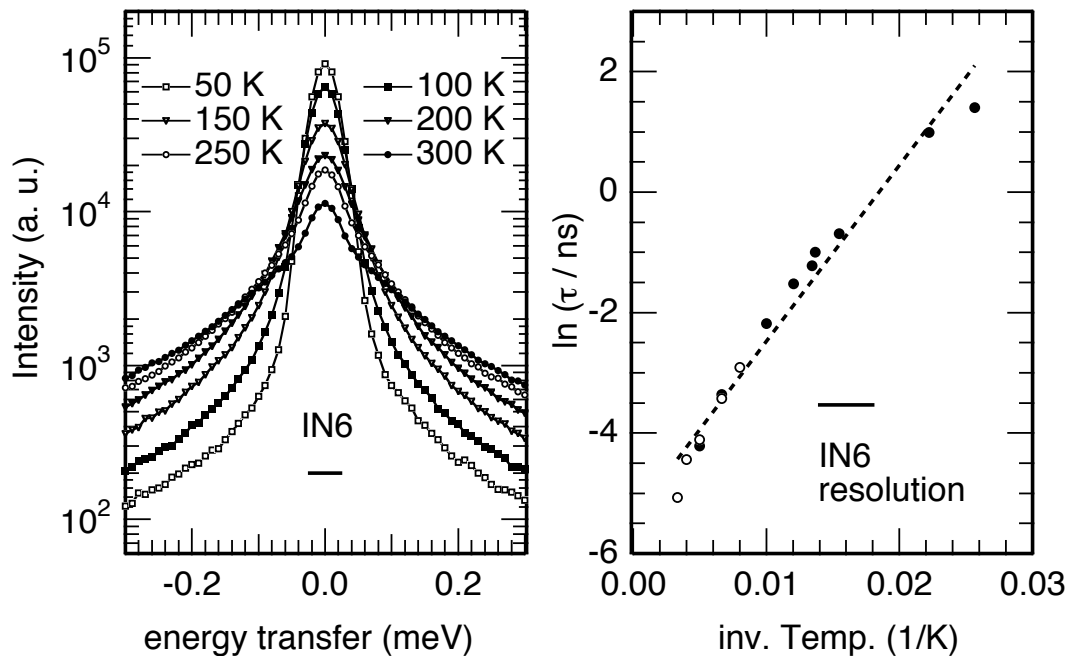


Figure 2. Top panel: the quasielastic scattering obtained at IN6. The bar represents the instrumental resolution (50 μ eV FWHM). Bottom panel: The relaxation times measured on IN11 and IN6 revealing Arrhenius nature. Error bars are smaller than point sizes. Also marked is the relaxation time corresponding to the IN6 instrumental resolution after Fourier transform.

Figure 3 shows the temperature dependence of the *diffuse* elastic magnetic scattering obtained by *xyz*-polarization analysis from the NSE experiment. It shows that, at low temperature, most of the intensity increase takes place at low q . There are two remarkable ‘kinks’ in the curves. The one at $T \simeq 1$ K is clearly linked to the spin ice freezing. The second one at $T \simeq 50$ K marks the onset of distinguished spatial correlations giving a significant intensity increase at low q . Surprisingly, magnetic scattering is very intense up to $T \simeq 800$ K.

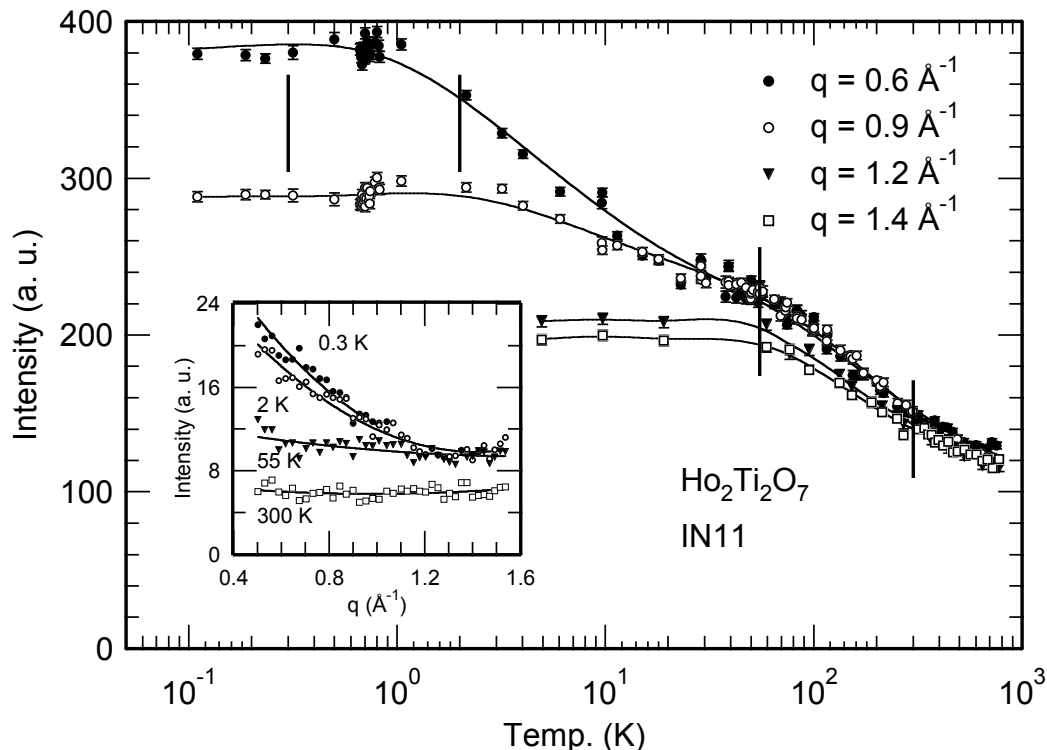


Figure 3. The temperature dependent magnetic scattering at different values of q . Lines are guides to the eye. The four vertical bars mark the temperatures at which the elastic scattering is shown as a function of q in the inset.

Figure 4 shows the parameter A and the value of $S(q, t)/S(q, 0)$ measured by NSE at $t = 1$ ns. Both curves have a plateau between $\simeq 2$ K and $\simeq 30$ K, which means that the relaxation in this range is *independent* of temperature and not Arrhenius-like. The Arrhenius process, whose parameters were fitted at higher temperatures, would rather give a level of spin correlation at $t = 1$ ns as shown by the dashed curve. The distinguished deviations below $\simeq 40$ K have two different origins. Firstly, the fact that $A < 1$, even at $T < 1$ K, proves the existence of a rapid process outside the NSE time window which cannot fully relax the spins. We suggest that this may be indicating small incoherent oscillations of the spins about their $\langle 111 \rangle$ easy axes. These, however, freeze towards very low temperature as well ($A = 0.95 \pm 0.01$ at $T \simeq 0.3$ K). At higher

temperature A slowly decreases, simply because the increasing weight of inelastic crystal field transitions in the scattering ($A = 0.60 \pm 0.03$ at 200 K) is not accounted for by a quasielastic scattering law. Secondly, and more important, another 10% loss of spin correlation at $t = 1$ ns indicates the existence of a different, *slower* relaxation process.

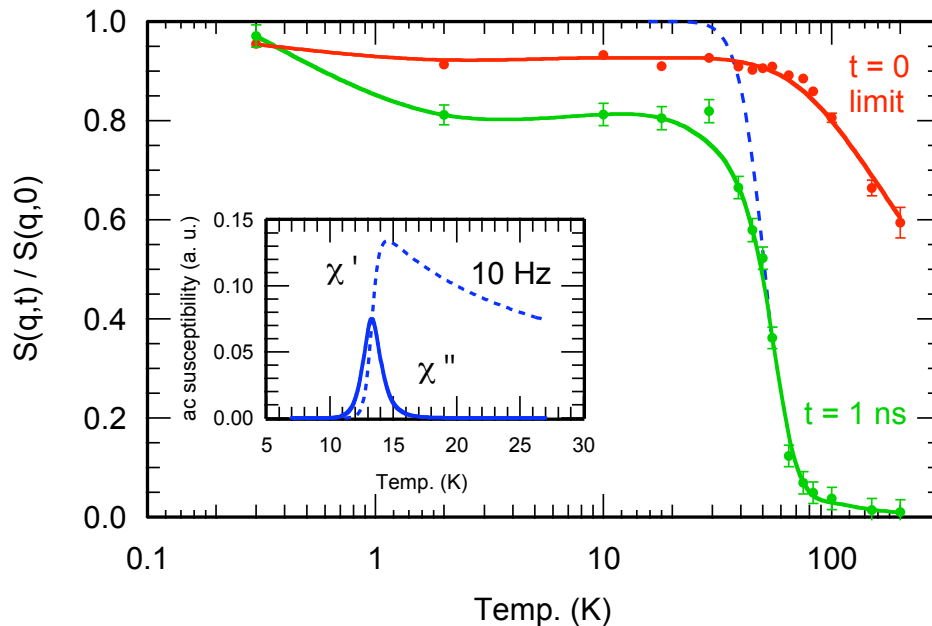


Figure 4. The $t = 0$ limit (parameter A) of the fit to the normalized intermediate scattering function $S(q, t)/S(q, 0)$ and the measured value at $t = 1$ ns. Lines are guides to the eye. The dashed curve shows what the correlation at $t = 1$ ns would be if only the fast process was present. Given the temperature dependence of its relaxation time, the inset shows the extrapolation into the ac susceptibility window (see text).

3.2. ac susceptibility

We now compare the spin echo results with ac susceptibility measurements. The generalized dynamic susceptibility corresponding to the measured exponential scattering function reads

$$\chi(q, \omega) = \chi(q) \cdot \left\{ \frac{\nu^2(T)}{\nu^2(T) + \omega^2} + \frac{i\omega\nu(T)}{\nu^2(T) + \omega^2} \right\}, \quad (2)$$

which allows extrapolation into the ac susceptibility window. In a good approximation one can set $\chi(q) \propto 1/T$ at low temperature. Inserting $\nu(T) = 1/2\tau(T)$ from the NSE measurement one finds that a peak in the ac susceptibility should appear around $T \simeq 15$ K. This is shown in the inset of Figure 4. However, such a peak hadn't been reported [6] in the literature before.

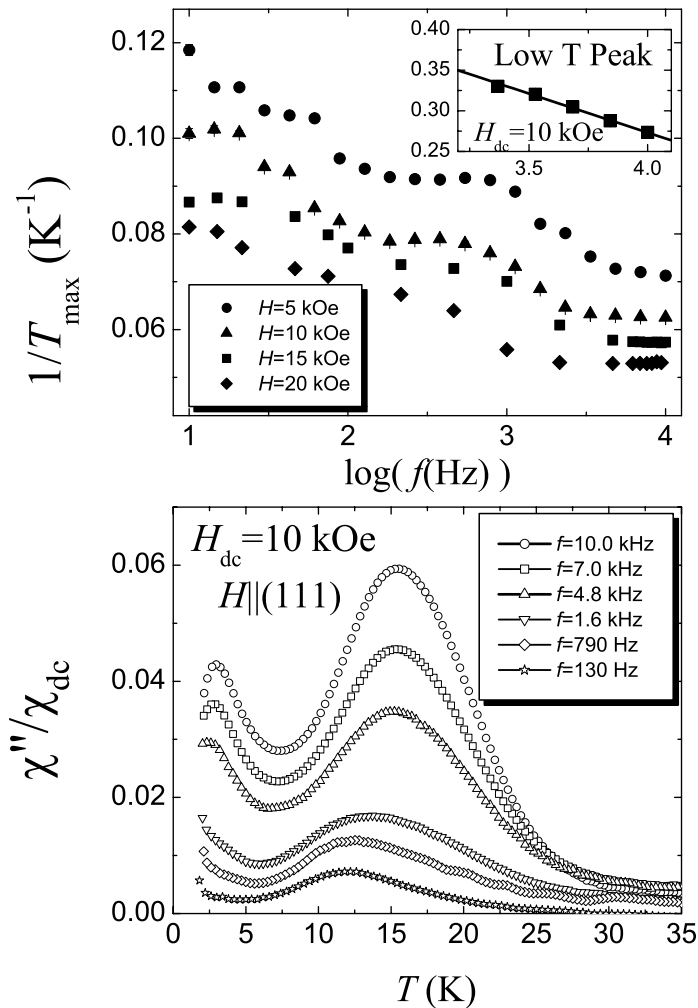


Figure 5. AC susceptibility data taken on a single crystal of $\text{Ho}_2\text{Ti}_2\text{O}_7$. Upper panel: the high temperature peak position as a function of $\log f$ at different fields. Lower panel: Frequency dependence of the ac susceptibility (imaginary part) measured in an applied dc field $B = 1$ T parallel to the $\langle 111 \rangle$ axis. Inset: Arrhenius behaviour of the low temperature feature in the same field.

Figure 5 shows the ac susceptibility data on a single crystal of $\text{Ho}_2\text{Ti}_2\text{O}_7$ in an applied field of $B = 1$ T. The expected peak at $\simeq 15$ K is clearly seen in a high magnetic field, but not in low field. Its frequency shift is consistent with the expected activation barrier of $\simeq 250$ K. Thus it is straightforward to conclude that this peak corresponds to the process that is seen in the NSE experiment. The frequency shift of the peak corresponding to the spin ice freezing at $T \simeq 1$ K (shown in the inset of Figure 4) indicates an energy barrier of $E_a = 24 \pm 1$ K and a characteristic time $\tau_0 = 22 \pm 5$ ns ($\Gamma_0 \simeq 2 \times 10^7$ Hz) at $B = 1$ T.

3.3. physical interpretation

The process seen in NSE is characterized by i) absence of q dependence of the scattering, suggesting a single-spin process, ii) a spin autocorrelation function which is exponential in time, and iii) it is thermally activated with an activation energy close to the first group of CEF levels. On the basis of these experimental observations we conclude that this process corresponds to spin flips between the two states of the ground state doublet. This process freezes out around $\simeq 15$ K. Since the ac susceptibility continues to increase below that temperature, there must be a second, different process, present at lower temperature. From the available data we conclude that this process is only weakly temperature dependent. Below $T \simeq 4$ K it becomes thermally activated with an attempt frequency of $\simeq 10^{10}$ Hz and activation barrier of $\simeq 30$ K [6] in low field. The latter value is closer to the other energy scale in the system, the dipolar interaction [3].

We suggest that this second, slower process is due to *quantum tunneling* of the spin between the two states of the ground state doublet. We identify the slowly fluctuating dipolar field at the rare earth site, created by the neighbouring spins, as the most likely origin of the quantum fluctuations. The transverse component of this field will create a finite rate of spin inversion, as long as the *mean field* is still zero. The gradual spin ice freezing below 4 K then corresponds to development of a mean field, which splits the Ho^{3+} ground state doublet, thus extinguishing the relaxation channel.

In this picture it can be understood why the 15 K peak is visible in DTO but much less apparent in HTO. Two different processes on different time and energy scales are revealed by two peaks in the ac susceptibility, provided the respective rates are not too similar. The latter is the case in HTO in low field, which is why the 15 K is not really visible. The effect of an externally applied magnetic field is that it slows down the slower process in HTO, thus revealing the 15 K peak (at $B = 1$ T, the attempt frequency is lowered to $\simeq 10^7$ Hz, see Figure 5). Assuming that our picture essentially holds for DTO as well, it is the slower intrinsic rate of the slow (quantum) process in that compound that makes the 15 K peak of the susceptibility more pronounced. Similarly, the effect of dilution on the spin ice dynamics [22] can be qualitatively understood. Dilution apparently speeds up the slow process, so that already at 15 K all relaxation is due to the slow process and the susceptibility peak naturally disappears. This is also consistent with a new result [28] that at *very low* concentration of the magnetic ions the 15 K reappears in DTO. At an increasing level of dilution, the slow quantum process will eventually go away when there are too few magnetic ions, because the dipolar field will become too low. The fast process, on the other hand, resulting from the crystal field, is unaffected by dilution, and should still be present even in the extreme case of a single magnetic ion in a crystal of $\text{Y}_2\text{Ti}_2\text{O}_7$.

Acknowledgments

The authors wish to thank S. Pujol for his help in setting up the low temperature equipment in the neutron scattering experiment. This work was supported by the Spallation Neutron Source Project (SNS). SNS is managed by UT-Battelle, LLC, under contract DE-AC05-00OR22725 for the U.S. Department of Energy.

References

- [1] Harris M J, Bramwell S T, McMorro D F, Zeiske T and Godfrey K W 1997 *Phys. Rev. Lett.* **79** 2554
- [2] Harris M J, Bramwell S T, Holdsworth P C W and Champion J D M 1998 *Phys. Rev. Lett.* **81** 4496
- [3] Bramwell S T and Gingras M J P 2001 *Science* **294** 1495
- [4] Siddharthan R, Shastry B S, Ramirez A P, Hayashi A, Cava R J and Rosenkranz S 1999 *Phys. Rev. Lett.* **83** 1854
- [5] Ramirez A P, Hayashi A, Cava R J, Siddharthan R and Shastry B S 1999 *Nature* **399** 333
- [6] Matsuhira K, Hinatsu Y, Tenya K and Sakakibara T 2000 *J. Phys.: Condens. Matter* **12** L649
- [7] Kadowaki H, Ishii Y, Matsuhira K and Hinatsu Y 2002 *Phys. Rev.* **B 65** 144421
- [8] Diep H T 1994 *Magnetic Systems with Competing Interactions: Frustrated Spin Systems* (World Scientific, Singapore)
- [9] Ramirez A P 1994, *Annu. Rev. Mater. Sci.* **24** 453
- [10] Gardner J S, Gaulin B D, Lee S H, Broholm C, Raju N P and Greedan J E 1999 *Phys. Rev. Lett.* **83** 211
- [11] Gardner J S, Ehlers G, Heffner R H and Mezei F 2001 *J. Magn. Magn. Mater.* **226-230** 460
- [12] Gardner J S, Dunsiger S R, Gaulin B D, Gingras M J P, Greedan J E, Kiefl R F, Lumsden M D, MacFarlane W A, Raju N P, Sonier J E, Swainson I and Tun Z 1999 *Phys. Rev. Lett.* **82** 1012
- [13] Champion J D M, Wills A S, Fennell T, Bramwell S T, Gardner J S and Green M A 2001 *Phys. Rev.* **B 64** 140407
- [14] Ehlers G, Casalta H, Lechner R E and Maletta H 2001 *Phys. Rev.* **B 63** 224407
- [15] Yelon W B, Cox D E and Eibschütz M 1975 *Phys. Rev.* **B 12** 5007
- [16] Farkas A, Gaulin B D, Tun Z and Briat B 1991 *J. Appl. Phys.* **B 69** 6167
- [17] Mao M, Gaulin B D, Rogge R B and Tun Z 2002 *Phys. Rev.* **B 66** 184432
- [18] Rosenkranz S, Ramirez A P, Hayashi A, Cava R J, Siddharthan R and Shastry B S 2000 *J. Appl. Phys.* **B 87** 5914
- [19] Bramwell S T, Harris M J, den Hertog B C, Gingras M J P, Gardner J S, McMorro D F, Wildes A R, Cornelius A L, Champion J D M, Melko R G and Fennell T 2001 *Phys. Rev. Lett.* **87** 047205
- [20] Harris M J, Bramwell S T, Zeiske T, McMorro D F and King D J C 1998 *J. Magn. Magn. Mater.* **177-181** 757
- [21] Matsuhira K, Hinatsu Y and Sakakibara T 2001 *J. Phys.: Condens. Matter* **13** L737
- [22] Snyder J, Slusky J S, Cava R J and Schiffer P 2001 *Nature* **413** 48
- [23] Snyder J, Slusky J S, Cava R J and Schiffer P 2002 *Phys. Rev.* **B 66** 064432
- [24] Mezei F, Pappas C and Gutberlet T 2003 *Neutron Spin Echo, Lecture Notes in Physics* vol 601 (Springer, Berlin)
- [25] Mezei F 1993 *Int. J. Mod. Phys* **B 7** 2885
- [26] Casalta H, Schleger P, Bellouard C, Hennion M, Mirebeau I, Ehlers G, Farago B, Dormann J L, Kelsch M, Linde M and Phillipp F 1999 *Phys. Rev. Lett.* **82** 1301
- [27] Schärpf O and Capellmann H 1993 *Phys. Status Solidi* **A 135** 359
- [28] Schiffer P 2003 private communication, to appear in the same volume of *J. Phys.: Condens. Matter*